Topical meeting on advances in reactor computations
Salt Lake City, Ut, USA
28-31 March 1983
CEA-CONF- 6715

EXPANSION AND COMPRESSION SHOCK WAVE CALCULATION IN PIPES WITH THE C.V.M. NUMERICAL METHOD

P. RAYMOND*, P. CAUMETTE**, G. LE COQ*, M. LIBMANN*

ABSTRACT

The Control Variables Method for fluid transients computations has been used to compute expansion and compression shock waves propagations. In this paper, first analytical solutions for shock wave and rarefaction wave propagation are detailled. Then after a rapid description of the C.V.M. technique and its stability and monotonicity properties, we will present some results about standard shock tube problem, reflection of shock wave, finally a comparison between experimental results obtained on the ELF facility and calculations is given.

* Département des Réacteurs à Eau
Service d'Etude des Réacteurs et de Mathématiques Appliquées
Laboratoire de Développement de Codes de Calcul
CEN/SACLAY 91191 GIF SUR YVETTE CEDEX

** Département des Réacteurs à Eau
Service de Technologie des Réacteurs à Eau
CEN/CADARACHE BP N° 1 13115 ST PAUL-LEZ-DURANCE

EXPANSION AND COMPRESSION SHOCK WAVE CALCULATION IN PIPES WITH THE C.V.M. NUMERICAL METHOD

INTRODUCTION

In nuclear engineering, thermal-hydraulic flow transients may induce expansion shock or compression shock waves in pipes. Calculation of shock waves and reflected shock waves are of interest in coupled fluid-structure interaction studies.

An inviscid, non heat-conducting and compressible fluid is described by the density ρ , the velocity $\vec{v}$ and the internal energy e . These basic variables satisfies the conservation laws of mass, momentum and energy. Thermodynamic quantities as entropy and pressure are functions of ρ and e.

For such a fluid two kinds of discontinuities occur . In "linear" discontinuity or contact discontinuity the pressure and the velocity are identical on the two sides of the contact discontinuity, however the densities, temperatures, energies and entropies have jump of values. In "non-linear" discontinuity or shock discontinuity, all the flow variables have jump of value. In contact discontinuity, velocity does not depend on the characterictics varying on both side of the discontinuity. The compression shock moves with a velocity which strongly depends on these characteristics.

From a physical view point, a theoretical analysis is more appropriate when an analytical solution can be obtained. Such calculations become too complicated when discontinuities are interacting and computation by numerical methods is needed.

Meanwhile, the use of numerical methods to compute discontinuities propagations in a fluid may lead to disappointing results :

- Occurence of parasitic oscillations near non linear discontinuities.

- Stretching of discontinuity profile.

- Calculation of non physical solutions.

In this paper, first, the propagation of shock waves in a perfect gas is discussed, then the Control Variable Method is described and some numerical results are presented for classical shock tube calculations and reflections of shock waves, finally calculations of pressure evolution on the ELF experiment are compared with measurements.

PROPAGATION OF SHOCK WAVES IN A PERFECT GAS

Consider two perfect gases, a driver gas at pressure P_4 , temperature T_4 and constant γ_4 , a test gas P_1, T_1, γ_1. At initial time a contact between

this two gases is performed. If P_4 is greater then P_1, a compression shock wave is propagating in the gas 1 and an expansion shock wave in the gas 4. Behind the compression wave a contact discontinuity will appear. At a given time the pressure and density distribution are schematically represented by the following figures.

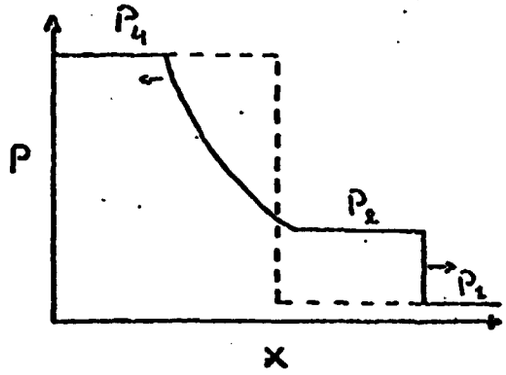

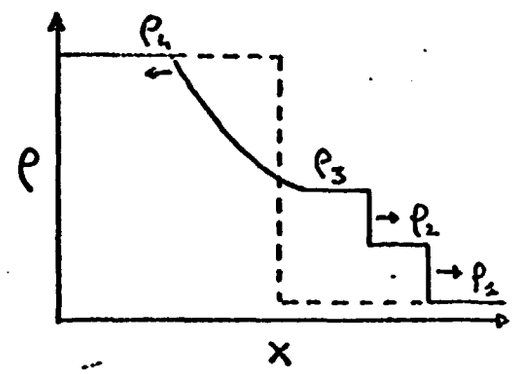

Let v_1 be the compression shock wave velocity and $M = \frac{v_1}{c_1}$ the Mach Number. The conservation equations leads to : [1, 2]

$$\rho_1 v_1 = \rho_2 v_2 \qquad (1)$$

$$P_1 + \rho_1 v_1^2 = P_2 + \rho_2 v_2^2 \qquad (2)$$

$$h_1 + \frac{1}{2} v_1^2 = h_2 + \frac{1}{2} v_2^2 \qquad (3)$$

h is the enthalpy $\quad h = \frac{P}{\rho} \frac{\gamma}{\gamma-1}$

By replacing h and v_2^2 in the equation (3) by their expression versus P_1, ρ_1, P_2, ρ_2 and γ_1 .

One obtains :

$$v_1^2 = \frac{2}{\rho_1} [(\gamma_1 - 1) P_1 - (\gamma_1 + 1) P_2]$$

as $\quad M = \frac{v_1}{c_1} = \frac{v_1}{\sqrt{\gamma_1 \frac{P_1}{\rho_1}}}$

The compression shock intensity is :

$$\frac{P_2}{P_1} = \frac{2\gamma_1}{\gamma_1+1} M^2 - \frac{\gamma_1 - 1}{\gamma_1 + 1} \qquad (4)$$

Considerer the rarefaction shock wave. The phenomenon is supposed isentropic so the density in this wave is obtained by :

$$\frac{P}{\rho^{\gamma_4}} = \frac{P_4}{\rho_4^{\gamma_4}}$$

From the sound velocity definition this relationship is equivalent to :

$$\rho = \rho_4 \left[\frac{c}{c_4}\right]^{\frac{2}{\gamma_4 - 1}}$$

The entropy being constant, this leads to the differential relationship :

$$c\, d\rho = -\rho\, dv$$

$$v = -\int \frac{c}{\rho} d\rho = \frac{2}{\gamma - 1}(c - c_4)$$

as

$$v_4 = 0 \Rightarrow c = c_4 - \frac{\gamma_4 - 1}{2} v$$

then :

$$\rho = \rho_4 \left(1 - \frac{\gamma_4 - 1}{\gamma_2} \frac{v}{c_4}\right)^{\frac{2}{\gamma_4 - 1}}$$

And

$$P = P_4 \left(1 - \frac{\gamma_4 - 1}{\gamma_2} \frac{v}{c_4}\right)^{\frac{2\gamma_4}{\gamma_4 - 1}}$$

Let v_2' be the velocity of the gas in the region 2.

The pressure variation in the rarefaction wave is

$$\frac{P_2}{P_4} = \left(1 - \frac{\gamma_4 - 1}{2} \frac{v_2'}{c_4}\right)^{\frac{2\gamma_4}{\gamma_4 - 1}} \qquad (5)$$

v_2' is the fluid velocity behind the shock, as the fluid in region 1 is at rest :

$$v_2' = v_1 - v_2$$

$$\frac{v_2}{v_1} = \frac{(\gamma_1 - 1) M^2 + 2}{(\gamma_1 + 1) M^2}$$

$$\text{so} \qquad v_2' = \frac{2(M^2 - 1)}{(\gamma_1 + 1) M^2}$$

$$\frac{v_2'}{c_4} = \frac{v_2'}{v_1} \frac{v_1}{c_1} \frac{c_1}{c_4} = \frac{2}{\gamma + 1} \frac{c_1}{c_4} \frac{M^2 - 1}{M} \qquad (6)$$

Now using (4), (5), (6), the Mach Number can be obtained from the initial conditions by the following implicit equation

$$\frac{P_4}{P_1} = \frac{P_2}{P_1}\frac{P_4}{P_2} = \frac{\gamma_1-1}{\gamma_1+1}\left[\frac{2\gamma_1}{\gamma_1-1}M^2 - 1\right]\left[1 - \frac{\gamma_4-1}{\gamma_1-1}\frac{c_1}{c_4}\frac{M^2-1}{M}\right]^{-\frac{2\gamma_4}{\gamma_4-1}} \qquad (7)$$

If the Mach number is calculated the expression (6) gives the velocity of contact discontinuity, relationships (4), (5) give the intensity of the compression and rarefaction shock waves.

The position of the extremities of the rarefaction shock wave may be calculated by considering the propagation of small pressure disturbances. The upper limit moves in the medium 4 with the velocity $v_4 + c_4 = c_4$ and the lower limit in the medium 3 with the velocity $v_3 - c_3 = v_2' - c_3$.

Let now calculate the physical parameters behind a reflected compression shock wave, $\tilde{P}_2$ is the pressure behind the reflected shock. The relative gas velocity behind the shock with respect to the gas ahead of it, is the same for the incident and the reflected shock wave, then (3) gives :

$$\tilde{v}^2 = (\tilde{P}_2 - P_2)\left[\frac{1}{\rho_2} - \frac{1}{\tilde{\rho}_2}\right] = [P_2 - P_1]\left(\frac{1}{\rho_1} - \frac{1}{\rho_2}\right)$$

Or

$$\frac{\rho_2}{\tilde{\rho}_2} = \frac{(\gamma_1+1)P_2 + (\gamma_1-1)\tilde{P}_2}{(\gamma_1-1)P_1 + (\gamma_1+1)\tilde{P}_2}$$

If the incident wave is strong $(P_2 \gg P_1)$

$$(\tilde{P}_2 - P_2)\left(\frac{1}{\rho_2} - \frac{1}{\tilde{\rho}_2}\right) \simeq P_2\left(\frac{1}{\rho_1} - \frac{1}{\rho_2}\right) \qquad \text{and} \quad \frac{\rho_2}{\rho_1} \simeq \frac{\gamma_1+1}{\gamma_1-1}$$

Note that this leads to :

$$\frac{\tilde{\rho}_2}{\rho_2} \simeq \frac{\gamma_1}{\gamma_1-1}$$

An order of magnitude of the reflected shock wave is given by :

$$\frac{\tilde{P}_2}{P_2} \simeq \frac{3\gamma_1-1}{\gamma_1-1}$$

THE CONTROL VARIABLE METHOD

In the last few years numerical methods have been developped for solving systems of non linear hyperbolic conservation laws.

There are several difficulties in solving such systems numerically. Inherent in any finite difference schemes is an assumption on the regularity of the solution. Typically, such schemes of order greater than 1 produce oscillations behind a shock, even if numerical artificial viscosity is added. In

récent papers G. SOD[3] and H.O. KREISS[4] have shown that in order to eliminate this oscillatory behaviour, numerical viscosity will be added, such as the accuracy of results is slightly the same as with first order schemes.

Basically the C.V.M. is a fully implicit numerical method developped for calculation of slow transients with large time steps greater than those imposed by classical Courant number limitations. Results obtained with this method has been presented in a previous paper[5]. . This method is briefly described.

The Control Variable Method solves the system of conservation laws for fluid dynamics in finite volumes. This method distinguishes between volume variables: mass, momentum and energy defined inside the volume, and surface fluxes of mass, momentum and energy. Volume variables then are discontinuous, but surface fluxes are continuous.

In any finite volume of a pipe with constant cross section, one-dimensionnal equations of fluid dynamics may be written in the following conservation form :

$$\frac{\partial}{\partial t}\rho + (\mathcal{G}_+ - \mathcal{G}_-)\frac{1}{h} = 0$$

$$\frac{\partial}{\partial t}\rho u + (\mathcal{P}_+ - \mathcal{P}_-)\frac{1}{h} = 0$$

$$\frac{\partial}{\partial t}\rho E + (\mathcal{E}_+ - \mathcal{E}_-)\frac{1}{h} = 0$$

Where

ρ is the density

ρu is the momentum

E is the total energy

$\mathcal{G}$ is the mass flux

$\mathcal{P}$ is the momentum flux

$\mathcal{E}$ is the energy flux

h is the mesh size ($h = V/S$).

The conservation principles are fulfilled by continuity of fluxes between volumes.

To close the system these fluxes are related to volume variables by relationships :

$$\mathcal{G} = \rho u$$

$$\mathcal{P} = P + \rho u^2$$

$$\mathcal{E} = \rho u (E + P/\rho)$$

Where P is the static pressure.

For a given flux between meshes i and $i+1$, the choice of volume variables needed to write previous relationships is made according to stability and entropy production rules.

To compute all the variables of a problem, first, a prediction of the momentum flux is performed which permits to obtain the momentum, then the mass fluxes. After solving the continuity equation density, pressure, and velocity are obtained for all meshes, then energy equation is solved. The comparison between the density obtained with the continuity equation $\tilde{\rho}$ and the density given by the state equation $\rho(P,e)$ allows to calculate a better value of the momentum flux by linearizing the equation :

$$\tilde{\rho} - \rho(P,e) = 0$$

This leads to solve the following second order partial differential equation.

$$\frac{\partial}{\partial t}\left[\frac{1}{c^2-u^2}\left[\frac{\partial \mathcal{P}}{\partial t} - 2u\frac{\partial \mathcal{P}}{\partial z}\right]\right] - \frac{\partial^2 \mathcal{P}}{\partial z^2} = -\frac{\partial}{\partial t}\left[\frac{\partial \rho}{\partial S}\Big|_P \frac{c^2}{c^2-u^2}\frac{\partial S}{\partial t}\right]$$

Iterations are carried out until a precision criterium on the densities difference is fulfilled.

STABILITY RULES

It can be prouved that density, mass flux and static pressure are solutions of a second order P.D.E., these equations are equivalent to equation (8).

To define fluxes of mass momentum an energy three criteria had to be satisfied.

a) Consistency criteria.

i.e ; if $h \to 0$ and $\Delta t \to 0$

$$\Rightarrow \quad \mathcal{G} \to \rho u$$
$$\mathcal{P} \to P + \rho u^2$$
$$\mathcal{E} \to \rho u\left(e + \frac{u^2}{2} + \frac{P}{\rho}\right)$$

b) Stability criterium : discretization will give for any volume a classical stable scheme on the second order PDE (8).

For instance if the fluid moves from mesh i to $i+1$.

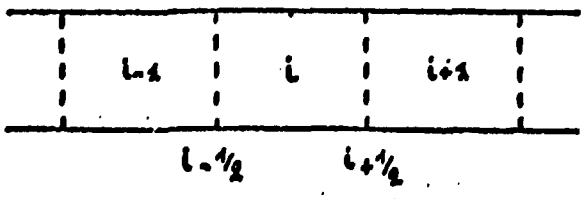

A fully implicit implicit and unconditionnaly stable scheme is obtained by definning at computational time t :

$$\text{Scheme 1} \begin{cases} \mathcal{G}^{t}_{i+1} = \rho^{t}_{i}\, u^{t}_{i} \\ \mathcal{P}^{t}_{i+1/2} = P^{t}_{i+1} + \mathcal{G}^{t}_{i+1/2}\, u^{t}_{i} \end{cases}$$

A more accurate implicit scheme is given by :

$$\text{Scheme 2} \begin{cases} \mathcal{G}_{i+1/2} = \rho^{t}_{i}\, u^{t}_{i} \\ \mathcal{P}^{t}_{i+1/2} = P^{t}_{i+1} + \mathcal{G}^{t}_{i+1/2} \dfrac{u^{t}_{i} + u^{t}_{i+1}}{2} \end{cases}$$

A semi implicit scheme stable only if Courant number $u \dfrac{\Delta t}{\Delta z} < 1$ is :

$$\text{Scheme 3} \begin{cases} \mathcal{G}^{t}_{i+1/2} = \rho^{t}_{i}\, u^{t}_{i} \\ \mathcal{P}^{t}_{i+1/2} = P^{t}_{i+1} + \mathcal{G}^{t-1}_{i+1/2}\, u^{t-1}_{i} \end{cases}$$

The third criterium is a dissipative criterium or entropy production rule .

ENTROPY PRODUCTION RULE

The second law of thermodynamic sets that entropy production will be positive or nul.

Let consider the differential relationship

$$T\, d\, S = de + P\, d\, \frac{1}{\rho}$$

The conservation of entropy can be expressed by

$$T\ \left(\frac{\partial \rho S}{\partial t} + \frac{\partial G S}{\partial z}\right) = \frac{\partial \rho e}{\partial t} + \frac{\partial G e}{\partial z} + P\, \frac{\partial u}{\partial z}$$

$$= -\ \left(\frac{\partial \rho \frac{u^2}{2}}{\partial t} + \frac{\partial G \frac{u^2}{2}}{\partial z}\right) + u\left(\frac{\partial \rho u}{\partial t} + \frac{\partial G u}{\partial z}\right) = \sigma(S)$$

With $\sigma(S) \geq 0$

This leads to express the discretization of cinetic energy terms of energy conservation equation from discretization of momentum equation. If entropy production rule is satisfied, the numerical solution obtained will have a physical sense. If a compression shock exists entropy production had to be equal or greater than physical entropy production due to the shock.

For the three previous scheme this leads to :

Scheme 1

$$\frac{1}{\Delta t}\left[\rho_i^t E_i^t + \rho_i^{t-1} E_i^{t-1}\right] + \frac{1}{h}\left[\mathcal{G}^t_{i+1/2} E_i^t - \mathcal{G}^t_{i-1/2} E_{i-1}^t\right] + \frac{1}{h}\left[P_{i+1}^t u_i^t - P_i^t u_{i-1}^t\right] = 0$$

With $E_i^t = e_i^t + \frac{1}{2}\left[u_i^t\right]^2$

And

$$\sigma(S) = \frac{1}{2}\left[\frac{\rho_i^{t-1}}{\Delta t}\left[u_i^t - u_i^{t-1}\right]^2 + \mathcal{G}^t_{i-1/2}\frac{1}{h}\left[u_i^t - u_{i-1}^t\right]^2\right]$$

Scheme 2

$$\frac{1}{\Delta t}\left[\rho_i^t E_i^t - \rho_i^{t-1} E_i^{t-1}\right] + \frac{1}{h}\left[\mathcal{G}^t_{i+1/2} E_i^{*t} - \mathcal{G}^t_{i-1/2} E_{i-1}^{*t}\right] + \frac{1}{h}\left[P_{i+1}^t u_i^t - P_i^t u_{i-1}^t\right] = 0$$

With $E_i^t = e_i^t + \frac{1}{2}\left[u_i^t\right]^2$

$$E_i^{*t} = e_i^t + \frac{1}{2}\left[u_{i+1}^t u_i^t\right]$$

and

$$\sigma(S) = \frac{1}{2}\rho_i^{t-1}\left[\frac{1}{\Delta t}\left(u_i^t - u_i^{t-1}\right)^2\right]$$

This scheme is less dissipative than first scheme.

Scheme 3

$$\frac{1}{\Delta t}\left[\rho_i^t E_i^t - \rho_i^{t-1} E_i^{t-1}\right] + \frac{1}{h}\left[\mathcal{G}^t_{i+1/2} E_i^{*t-1} - \mathcal{G}^t_{i-1/2} E_{i-1}^{*t-1}\right] + \frac{1}{h}\left[P_{i+1}^t u_i^t - P_i^t u_{i-1}^t\right] = 0$$

With $E_i^t = e_i^t + \frac{1}{2}\left[u_i^t\right]^2 \frac{\rho_i^{t-1}}{\rho_i^t}$

$$E_i^{*t-1} = e_i^{t-1} + \frac{1}{2}\left[u_i^{t-2}\right]\frac{\mathcal{G}^{t-1}_{j+1/2}}{\mathcal{G}^t_{j+1/2}}$$

and

$$\sigma(S) = \frac{1}{2}\left\{\left(u_j^t - u_j^{t-1}\right)^2\left[\frac{\rho_j^{t-1}}{\Delta t} - \frac{\mathcal{G}^{t-1}_{j-1/2}}{\Delta z}\right] + \frac{\mathcal{G}^{t-1}_{j-1/2}}{\Delta z}\left[u_{j-1}^{t-1} - u_j^t\right]^2\right\}$$

$\sigma(S)$ can be negative for $u\,\frac{\Delta t}{\Delta z} > 1$

SHOCK TUBE STANDARD PROBLEM

A one meter shock tube with following discontinuous initial condition at abciss .5m was considered

$0 < x < .5$: $P_1 = 1$, $\rho_1 = 1$, $e_1 = 2.5$ — $.5 < x < 1$: $P_4 = 0.1$, $\rho_4 = 0.125$, $e_4 = 2.$

The isentropic exponent of perfect gas is : $\gamma = 1.4$.

From relationships obtained in previoux paragraph following quantities can be computer.

- Velocity of the compression shock : $v_1 = 1.75$
- Intensity of the compression shock : $\frac{P_2}{P_1} = 0.3026$
- Velocity of the contact discontinuity : $v_2 = 0.9256$
- Velocity of the upper limit of the rarefaction wave

$$-c_4 = -1.193$$

- Velocity of lower limit of the rarefaction wave

$$v_3' - c_3 = -0.075$$

Computation have been performed with fully implicit and semi-implicit schemes. In calculations the mesh size was $h = 0.01$ and the time step was taken to be such as.

$$\text{Max}\ \{(u + c)\ \frac{\Delta t}{h}\} = 1 \quad \Rightarrow \quad \Delta t = 5\ 10^{-3}5$$

Results at time $t = 0.15$ s are given in figure 1 and figure 2.

The studied schemes 1 and 3 do not produce any oscillation or non pysical behaviour as overshoot and undershoot near shocks. This is due to numerical dissipation (Fig. 3 and Fig. 4) due to discretization.

Scheme 2 produce a slight overshoot behind the compression shock which is reduced by reducing the mesh size and the time step. This will be considered as a non-physical result Scheme 2 does not produce sufficient dissipation to compute a shock (Fig. 5).

Even if semi implicit scheme gives best results than the fully implicit scheme. These two numerical methods stretch discontinuities profiles. It may be noticed that transition of contact discontinuity occupies more meshes than compression shock for all computations.

COMPUTATION OF SHOCK WAVE REFLECTION

To study reflection of compression shock wave on closed ends of pipe a second numerical test has been performed. A four meter closed pipe was modeled using eighty 0.05 m meshes. The pipe was initially filled of gas

with constant isentropic exponent ($\gamma = 1.4$). An initial discontinuity of pressure is imposed at abscisse $x = 3.m$

$0 < x < 3\,m \quad P = 12.\ MPa$

$3\,m < x < 4\,m \quad P = 0.1\ MPa$

For such a pressure discontinuity the initial compression shock has an intensity of about $\Delta P \simeq .2MPa$ and the rarefaction wave accelerates the gas until supersonic velocity (600 m/s) (Fig.6). Incident compression shock is reflected on the upper end of the pipe and produces an important second shock moving from upper extremity to lower. Behind this second shock the gas internal energy increases sharply near $x = 4$ m and the gas is at rest. The rarefaction wave is not reflected, and pressure at lower extremity decreases slowly. Due to the nul velocity of gas behind this shock ; (Fig. 7) there is no reflected shock on the lower extremity of the pipe. Meanwhile a new rarefaction wave is produced at the other extremity and this induces a new compression shock which will be reflected but with smaller intensity than for second shock.

Figure 8 shows the evolution of the pressure in the pipe and one can see that same phenomena as above described occurs periodically with a decreasing intensity for the reflected compression shock.

It can be noted that the calculation of reflected shock wave with non-monotoneous numerical schemes, will amplify oscillations inherent in such schemes.

CALCULATION OF ELF EXPERIMENTS

The ELF facility (Fig. 9) is devoted to study circonferential break propagation. A 1.5 m test section is linked to a 30.5 m pressurized pipe. A circonferential default in the test section a 1.38 m will initiate a circonferential break. At initial time, a rupture disk between test section and pipe is broken, a fast pressure transient is induced and generates the small break. Pressure is measured on various locations on the pipe.

For the studied run (n° 18) [6], the pressure in pipe is : 12.25 MPa and in test section : 0.1 MPa. The gas (air) is at same temperature ($T = 30°C$). The area of the created break is $183.4\ 10^{-6}\ m^2$.

Pressure measurements (Fig. 10, 11) show a periodic behaviour, a large pressure undershoot follows step with constant pressure.

To compute this experiment, it was assumed that the break is instantaneously created. The break was modeled by a loos of mass, momentum and energy in a cell, the air loss velocity is taken to be equal to sound velocity at atmospheric pressure.

The Figure 12 shows the pressure evolution obtained by calculation at same location than experimental measurement. Calculations of pressure undershoot intensity, pressure levels are and periodicity of the phenomena are in good agreement with experimental data.

The Figure 13 shows the same calculation without break, by comparing

this two results one can conclude that pressure levels will depend on the break flow rate.

CONCLUSIONS

In this paper, the ability to compute compression shock wave and rarefaction wave propagation by the Controle Variable Methodhas been shown. Further improuvements have to be made in order to reduce the numerical strenching of discontinuities by using antidiffusion methods. Also, calculations of multi-dimensional shock propagation will be performed.

REFERENCES

[1] L.D. LANDAU, E.M. LIFSHITZ "Mécanique des Fluides" Editions MIR.

[2] Y.B. ZEL'DOVICH, Y.P. RAIZER, "Physics of Shock Waves and Hight Temperature Hydrodynamic Phenomena". Academic Press (New-York and London 1966).

[3] G.A. SOD, "A Survey of Several Finite Difference Methods for Systems of Non linear Hyperbolic Conservation Laws". Journal of Computational Physics 27, 1-31 (1978).

[4] H.O. KREISS, "Numerical Solution of Conservation Laws".

[5] G. LE COQ, "The Triton Computer Code - Finite Difference Methods for 1-D Single or Two Fluid Transient Computation". ANS ENS Topical Meeting on Advances in Mathematical Methods for the Solution of Nuclear Engineering Problems. Munchen 1981.

[6] P. CAUMETTE, "Private Communication".

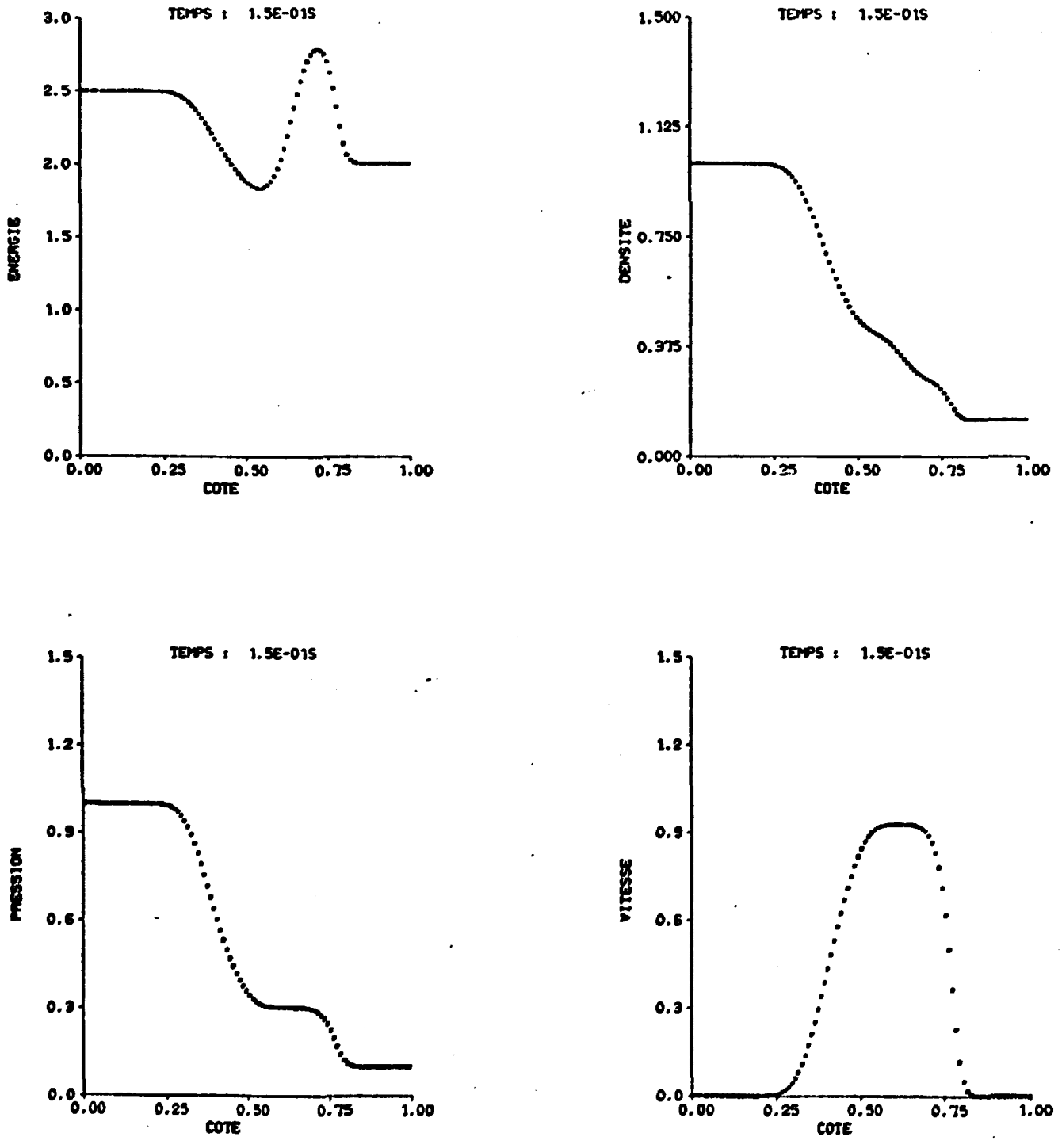

Fig. 1 : Standard Shock Tube Problem : Results at time .15 s computed with the fully implicit scheme (Scheme 1)

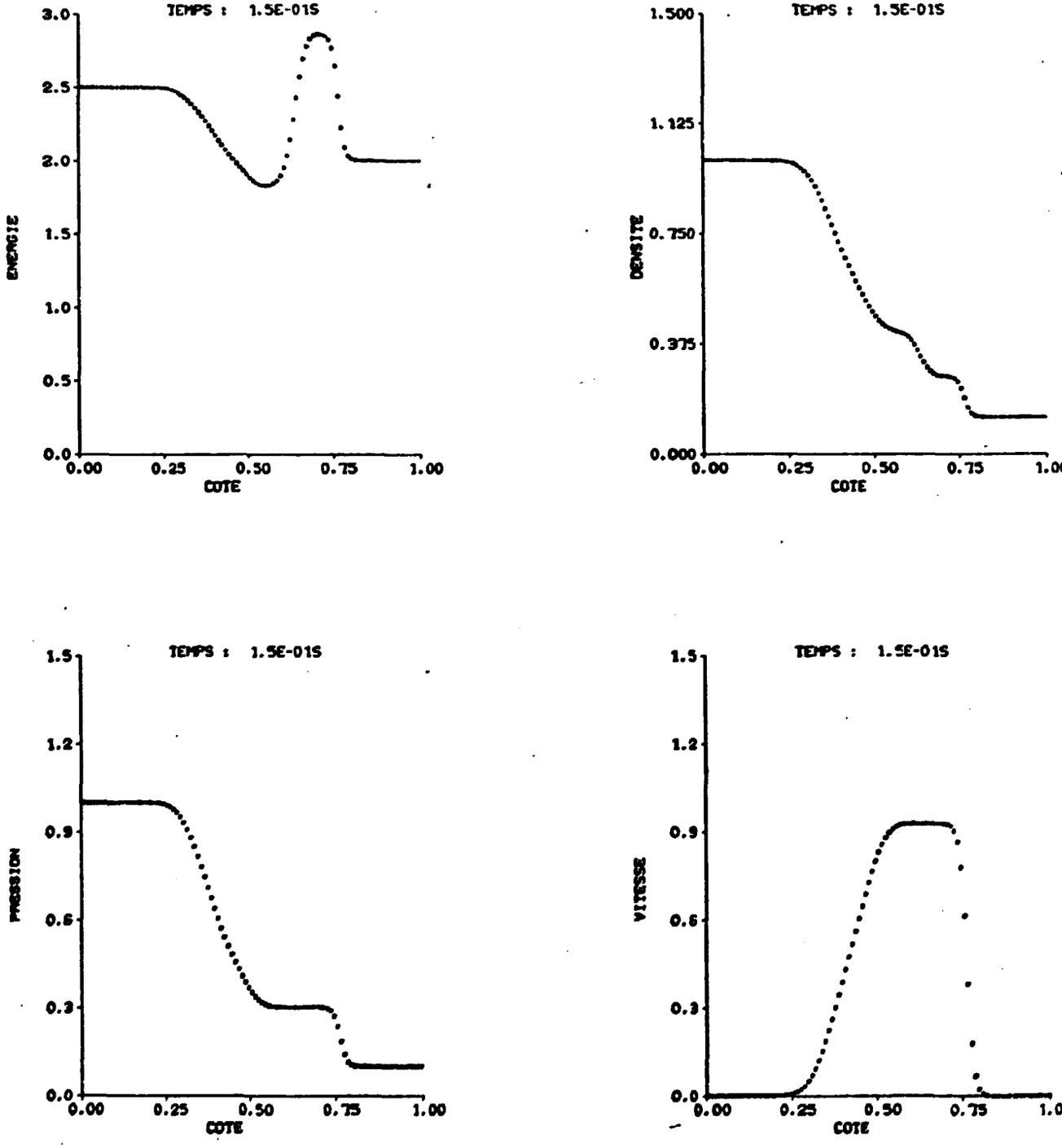

Fig. 2 Standard Shock Tube Problem : Results at time ·15 s computed with the semi-implicit scheme (Scheme 3).

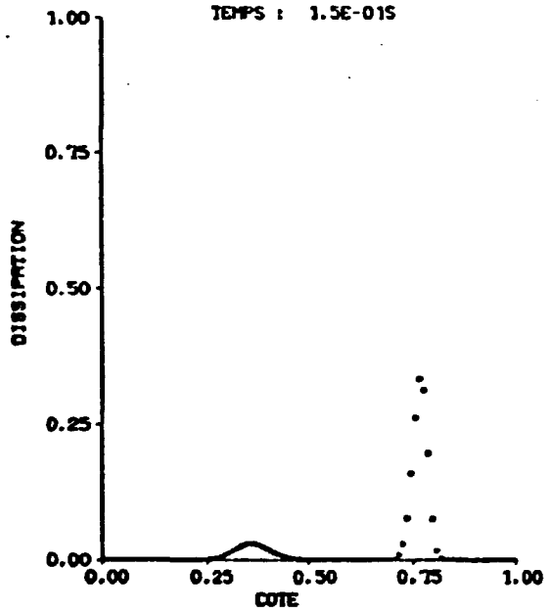

Fig. 3 Numerical dissipation for fully implicit scheme

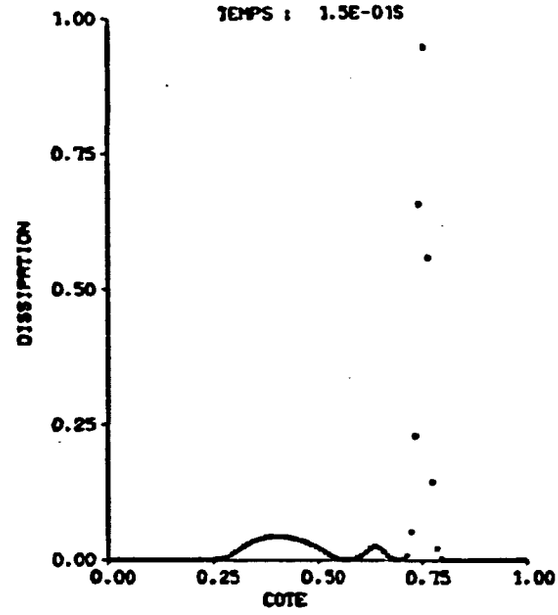

Fig. 4 Numerical dissipation for semi-implicit scheme

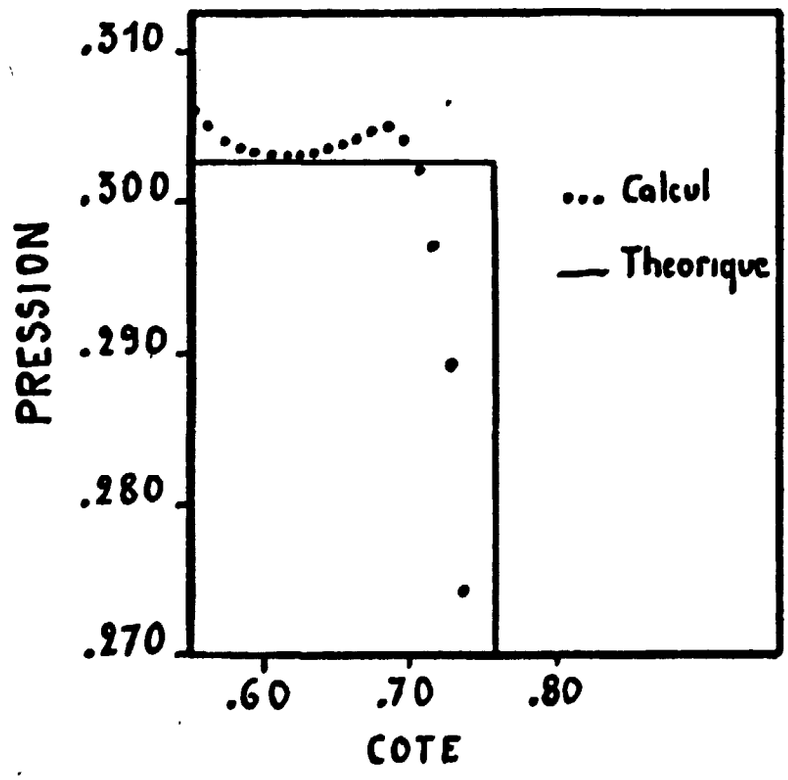

Fig. 5 Calculation of Compression Shock with scheme 2

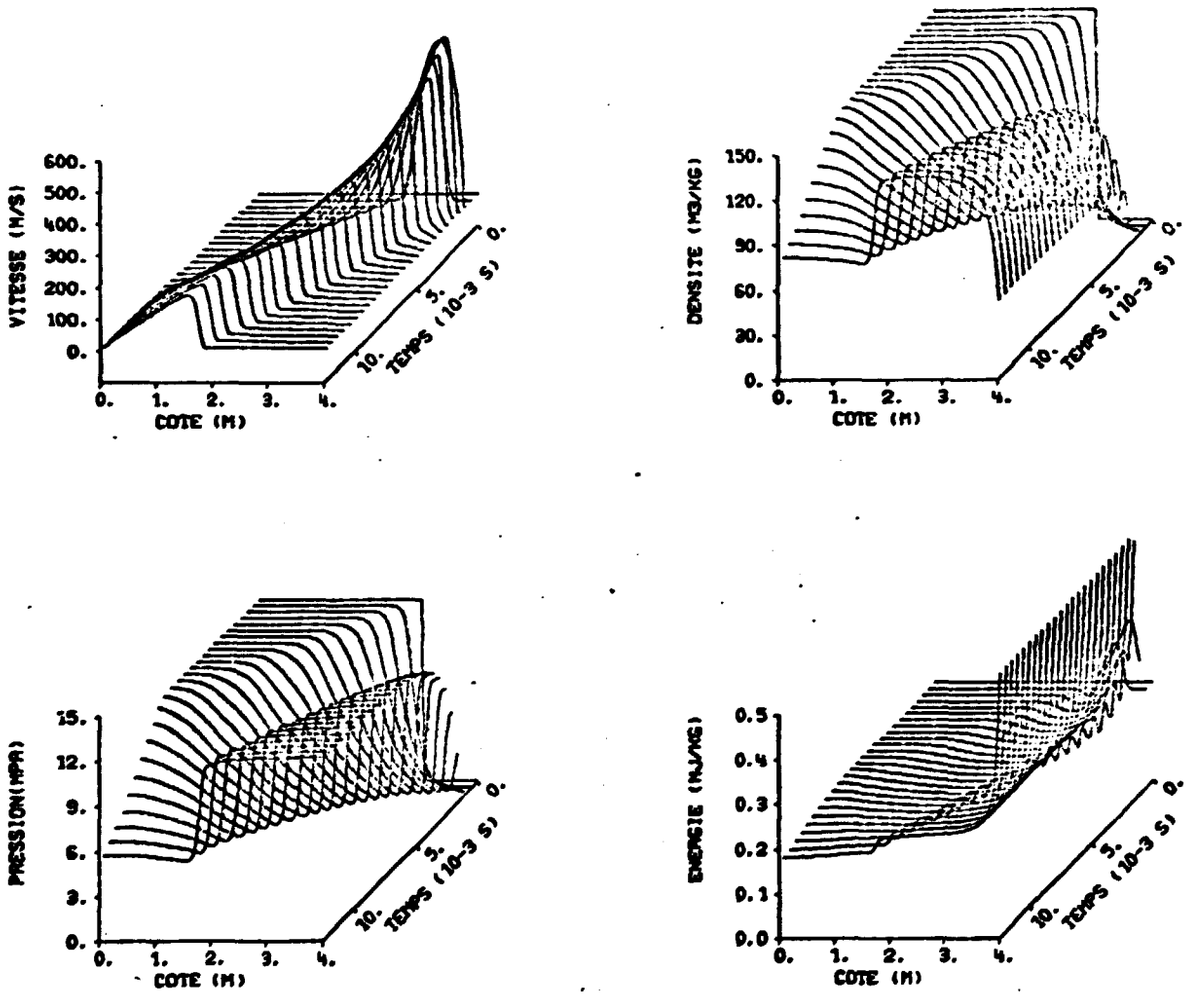

Fig. 6 : Reflection of Shock wave : Evolution of Flow parameters
From $t = 0.s$ to $t = 12.5 10^{-3} s$

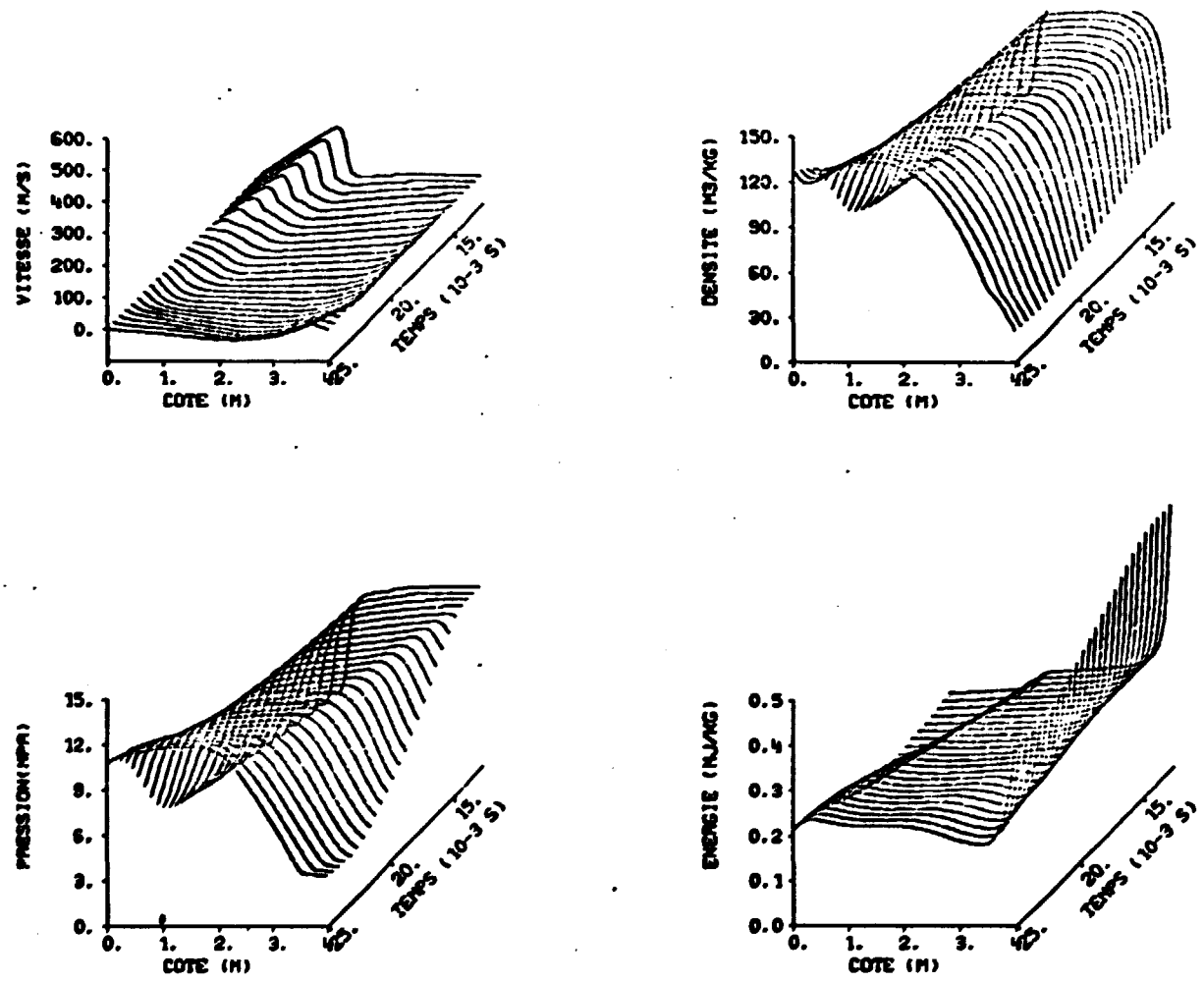

Fig. 7 : Reflection of Shock wave : Evolution of flow parameters
From $t = 12.5\ 10^{-3}$s to $t = 25.\ 10^{-3}$s

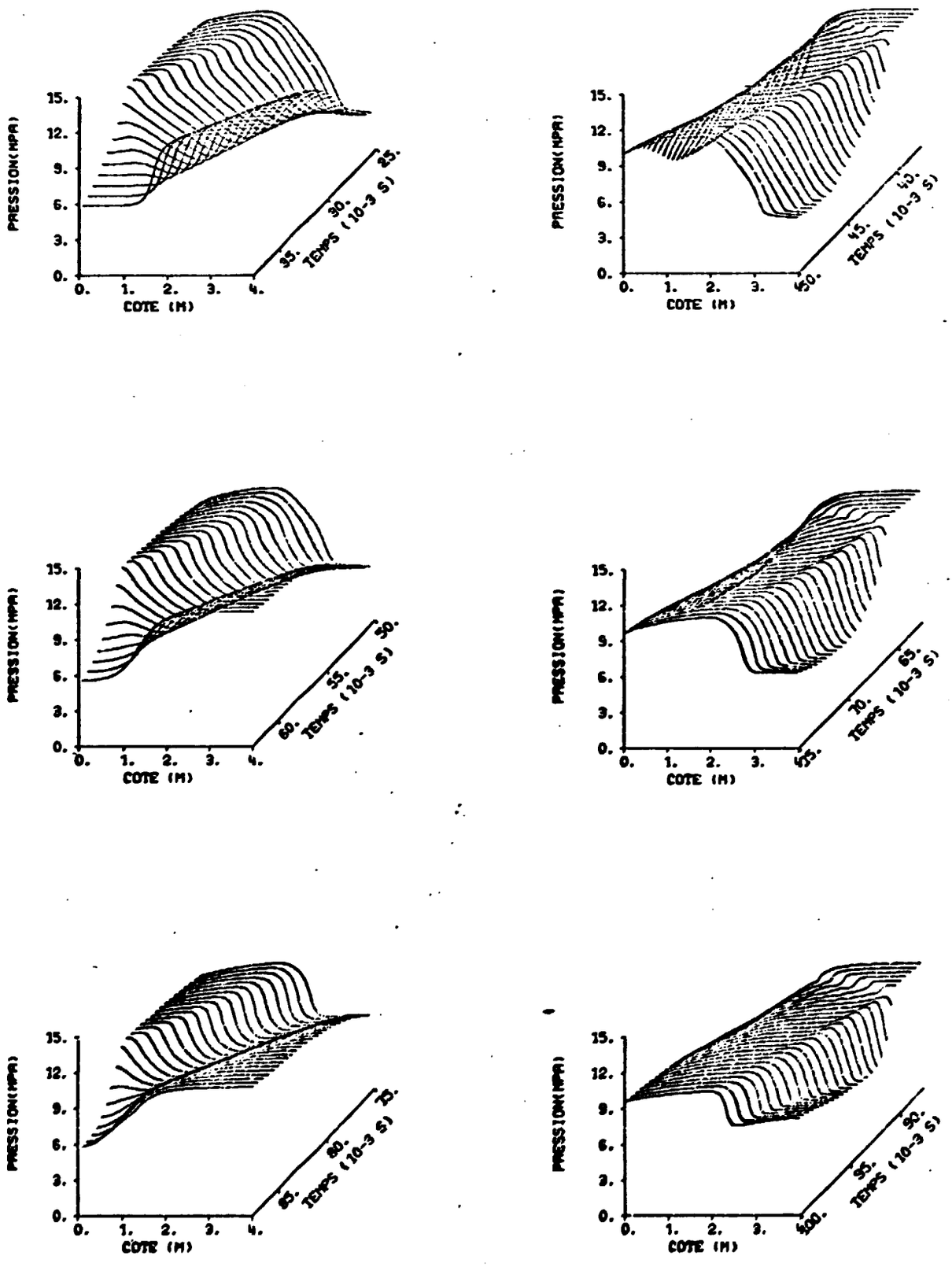

Fig. 8 : Reflection of Shock wave : Evolution of Pressure profile in the pipe From $t = 25\ 10^{-3}$ s to $t = 0{\cdot}1$ s

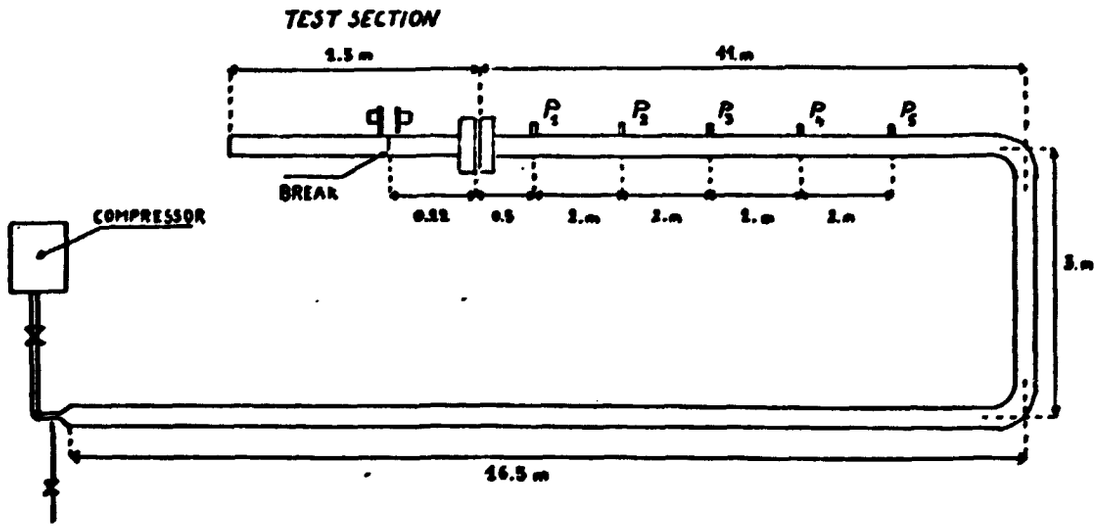

Fig. 9 : ELF experimental Facility : Schematic drawing of the Facility and location of pressure tapping.

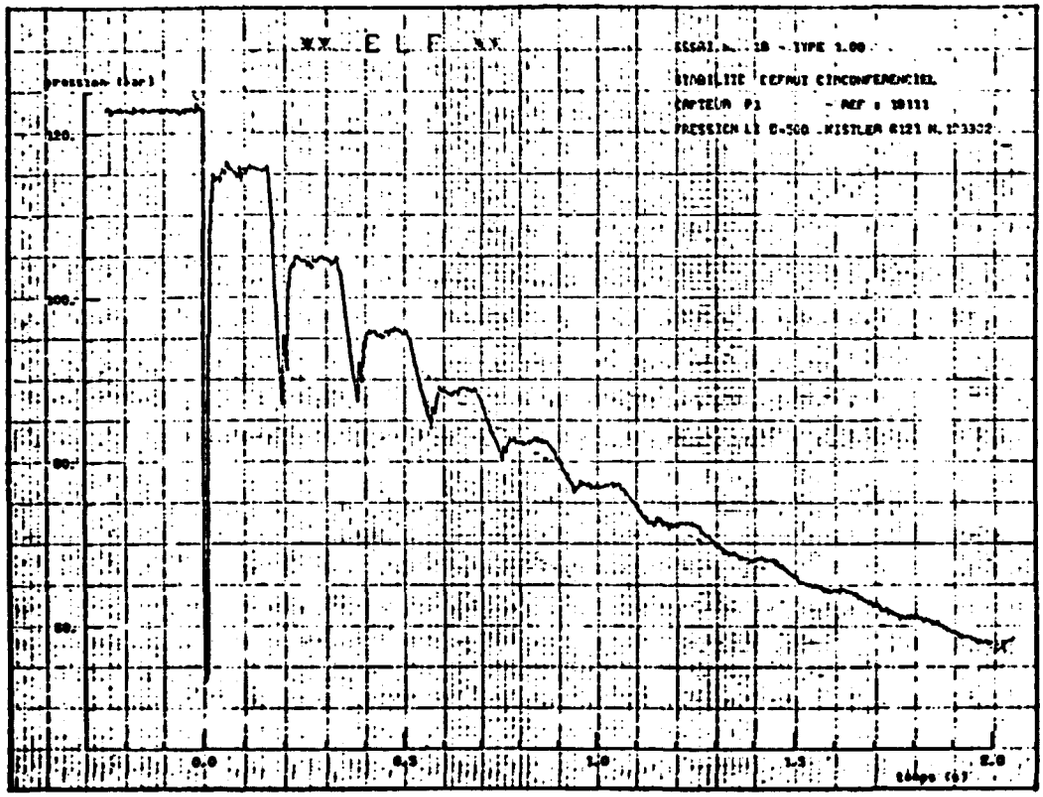

Fig. 10 : ELF experimental Facility : Typical pressure transient for run n° 18 (Pressure tap : P_1)

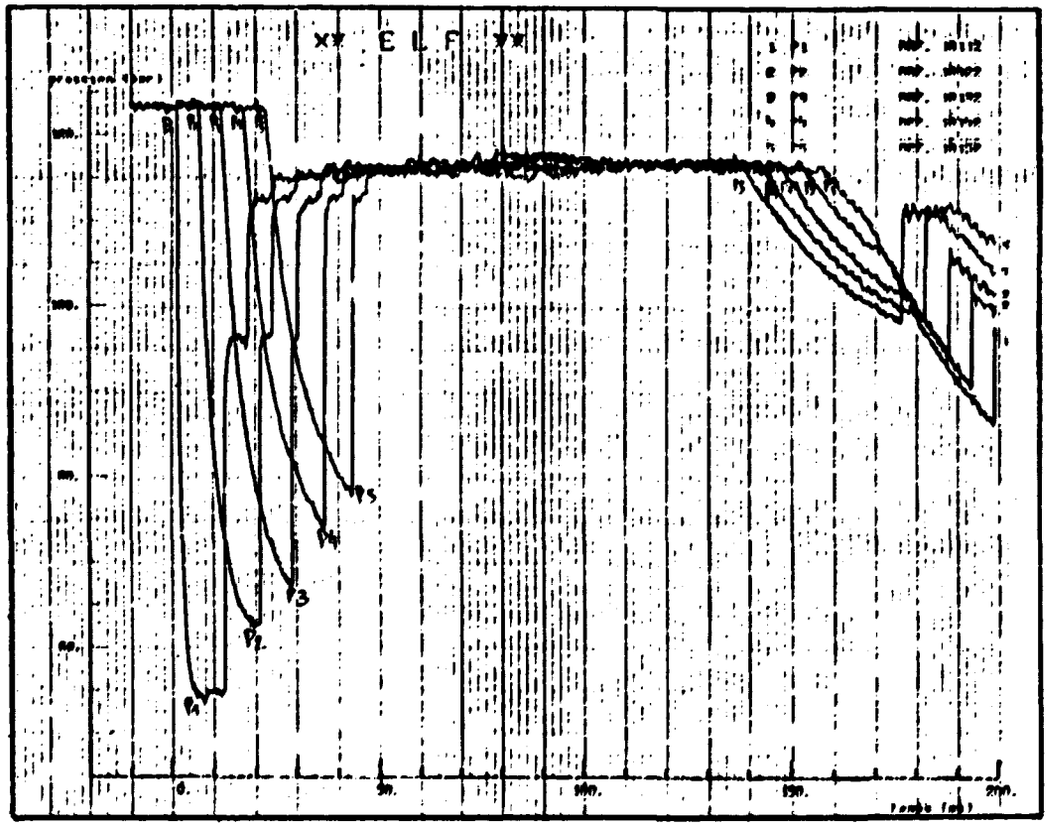

Fig. 11 ELF experimental Facility : Typical pressure transient for various pressure taps.

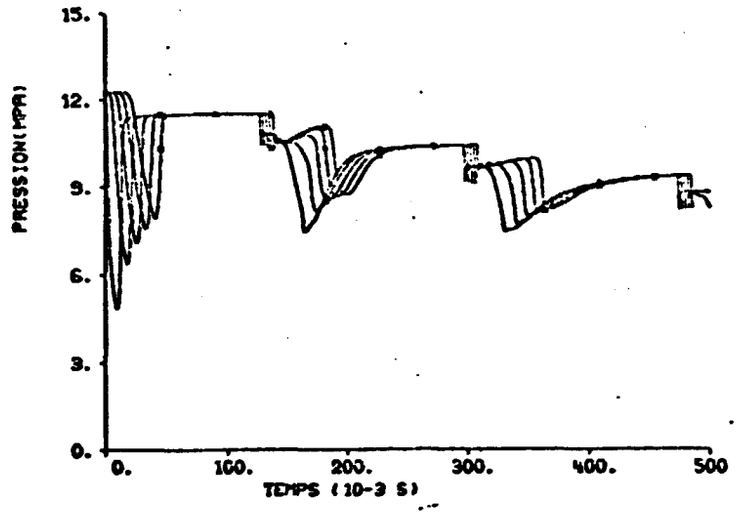

Fig. 12 : Computed pressure transient for ELF run n°18

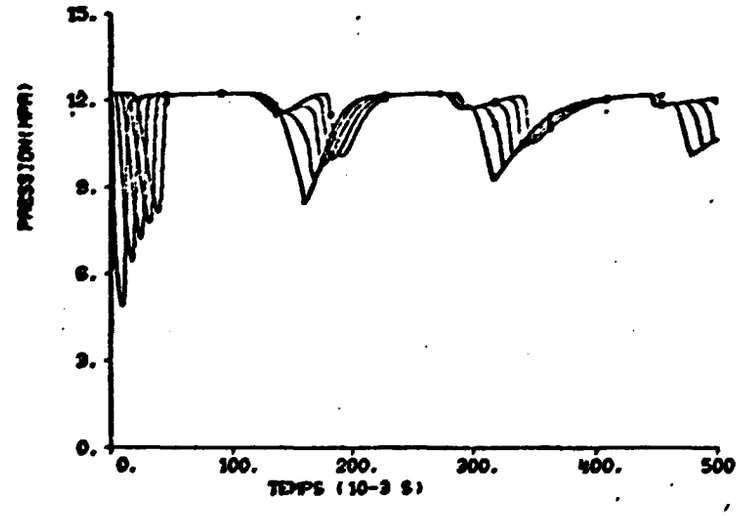

Fig. 13 : Computed pressure transient without break.